THE JOURNAL OF PHYSICAL CHEMISTRY B

ARTICLE

pubs.acs.org/JPCB

Diffusion and Interfacial Transport of Water in Nafion

Qiao Zhao, Paul Majsztrik, and Jay Benziger*

Department of Chemical and Biological Engineering and Department of Chemistry, Princeton University, Princeton, New Jersey 08544, United States

Supporting Information

ABSTRACT:

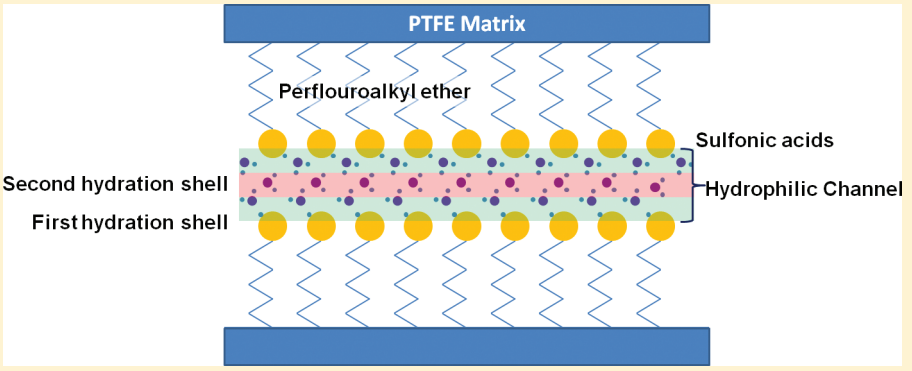

Water absorption, membrane swelling, and self-diffusivity of water in 1100 equivalent weight Nafion were measured as functions of temperature and water activity. Free volume per water at 80 °C, determined from water uptake and volume expansion data, decreases with water content in the membrane from 12 cm^3/mol at $\lambda = 0.5$ H_2O/SO_3 to 1.5 cm^3/mol at $\lambda = 4$. The change in free volume with water content displays a transition at $\lambda = 4$. Limiting water self-diffusivity in Nafion was determined by pulsed gradient spin echo NMR at long delay times. The limiting self-diffusivity increases exponentially with water activity; the rate of increase of diffusivity with water content shows a transition at $\lambda = 4$. The tortuosity of the hydrophilic domains in Nafion decreased from 20 at low membrane water activity to 3 at $\lambda = 4$. It suggested a change in the connectivity of the hydrophilic domains absorbed water occurs at $\lambda \sim 4$. The diffusivity results were employed to separate the contributions of diffusional and interfacial resistance for water transport across Nafion membranes, which enabled the determination of the interfacial mass transport coefficients. A diffusion model was developed which incorporated activity-dependent diffusivity, volume expansion, and the interfacial resistance, and was used to resolve the water activity profiles in the membrane.

INTRODUCTION

Polymer electrolyte membrane (PEM) fuel cells are a promising type of energy conversion device. For most of the conventional PEMs, the presence of water in the membrane is essential for achieving high proton conduction.[1−3] Water is produced at the cathode and must be absorbed and transported across the membrane. Knowledge of the kinetics of water sorption and transport in polymer electrolyte membranes is essential to optimize the design and operation of fuel cells.

Currently, the most effective membrane for a PEM fuel cell is Nafion. It is a perfluorosulfonated random copolymer with a tetrafluoroethylene backbone and perfluoroalkyl ether side chains terminated by sulfonic acid groups. Nafion microphase separates into hydrophilic domains of sulfonic acid groups and absorbed water imbedded in a hydrophobic matrix of tetrafluoroethylene (TFE) and perfluoroalkyl ether (PFA). Water and protons are transported through the network of hydrophilic domains. The hydrophilic domains swell and restructure as water is absorbed into Nafion, which changes the effective diffusion coefficient.

Water transport through Nafion has been extensively investigated for three decades by several different methods. Most investigators assumed that the rate of water transport was primarily controlled by diffusion.[4−8] However, the water diffusivities determined by different methods reported values that varied by more than 10^3 cm^2/s. In an effort to reconcile these differences, our group studied absorption, desorption, and permeation of water in Nafion membranes of different thicknesses and showed that depending on the activity and phase, water permeation, and sorption may be limited by interfacial mass transport, diffusion, or polymer swelling dynamics.[9]

Steady-state water transport across Nafion membranes is independent of membrane thickness when liquid water was present at one interface, but the transport scales inversely with membrane thickness when both interfaces were exposed to water vapor. These results suggested the rate-limiting step for water

Received: August 17, 2010
Revised: February 1, 2011
Published: March 03, 2011

transport was interfacial transport at the vapor/membrane interface when liquid water was present at one interface, but the rate-limiting step was diffusion across the membrane when vapor was present at both interfaces.[10] Monroe at al. developed a "vaporization-exchange" model with a boundary condition that accounts for interfacial vaporization kinetics to explain the interfacial transport at a vapor/Nafion interface.[11] Majsztrik et al. found that the effective water diffusion coefficient decreased with decreasing water activity, causing diffusion to become rate limiting at low water activity.

The goal of the present study is to quantify the effect of water activity in Nafion on both water diffusion and interfacial transport. Pulse field gradient spin echo nuclear magnetic resonance (PGSE-NMR) is the most reliable technique for self-diffusion measurements because it is not complicated by interfacial transport or kinetics of polymer swelling. Previous NMR studies have reported diffusivities of water in Nafion that varied from 10^{-5}–10^{-6} cm^2/s; the water diffusion coefficient increased modestly with increasing water activity.[12−15] Water diffusion coefficients measured by NMR predict much larger transport rates across Nafion membranes than have been measured experimentally.

We report here a systematic series of experiments measuring water absorption, linear expansion coefficient, and self-diffusivity of water as functions of water activity and temperature. The results provide the first direct measures of free volume and tortuosity of the hydrophilic domains associated with water sorption in Nafion. The detailed measurements of water diffusion as a function of water activity coupled with previous measurements of water permeation were able to separate the contributions of diffusion and interfacial transport of water across Nafion membranes.

EXPERIMENTAL SECTION

Membrane Preparation. Extruded Nafion, equivalent weight 1100 (EW = mass of polymer/mol HSO_3), was purchased from Ion Power and treated following the standard cleaning protocol developed in our lab for making reproducible Nafion films: anneal for 2 h at 80 °C in vacuum for 2 h, boil 1 h in 3% H_2O_2 solution, boil 1 h in deionized (DI) water, boil 1 h in 0.5 M sulfuric acid, and boil 1 h in DI water twice. The vacuum annealing is necessary to erase memory of membrane history. Membranes used for PGSE-NMR were ion-exchanged with 0.1 M EDTA (ethylenediaminetetraacetic acid) solution before boiling in sulfuric acid. This step removed paramagnetic impurities, such as Na^+ ions which can significantly shorten spin−lattice relaxation time (T_1) of water in the membrane.[16] The resulting clean and protonated Nafion was dried under compression between filter papers under ambient conditions for 2 days.

Equilibrium Water Absorption Experiments. The equilibrium mass uptake by Nafion was measured in an isothermal pressure vessel, similar to the device previously described by Yang et al.[17] A Nafion sample was mounted inside a vacuum container between two clamps. The vessel was placed in a temperature controlled oven. The vessel was evacuated to a base pressure of 10^{-6} bar. 5−25 μL aliquots of water were sequentially introduced to the vessel. The water was allowed to equilibrate for 30−60 min, until the pressure stabilized. The difference between the moles of water injected and the moles of water vapor in the vessel was equal to the water absorbed by the membrane, and the pressure in the vessel was equal to the water vapor partial pressure. Recording the pressure as a function of volume of water injected provided the measure of the moles of water absorbed as a function of the water activity. Water uptake was measured at 50, 60, and 80 °C.

Equilibrium Swelling Strain. Equilibrium swelling strain of Nafion due to water uptake from vapor was measured using a custom creep instrument with an environmental chamber.[18] Cleaned and dried Nafion membranes were cut into 0.64 cm wide strips and then clamped in the jaws of the instrument to give a gauge length of approximately 2.54 cm. The film was dried in situ at 80 °C for over 2 h in a purge of dry N_2. A small stress of ∼0.1 MPa was applied (enough to pull the film taught, but not enough to induce measurable creep). A step change in temperature and/or water activity was introduced and the length of the sample was monitored as a function of time while the temperature and water activity of the environmental chamber was held fixed. The final length was recorded when a steady-state length was reached. (Steady state was defined as when the rate of linear expansion was less than 0.1% per hour, $d\varepsilon/dt < 0.001\ h^{-1}$.) Depending on the temperature and water activity, the time needed to reach steady state took anywhere from 10 min to over 24 h. Equilibrium swelling strain was measured at 30, 40, 50, 80, and 98 °C from water activity of 0−0.95 at intervals of ∼0.1. Swelling strain was calculated with reference to dry Nafion at 23 °C.

PGSE-NMR. Cleaned Nafion membranes were cut into strips of 5.1 cm × 0.25 cm and inserted into NMR tubes. The NMR tubes used were cut to 7.6 cm long and had both ends open to fit in the environmental chamber and to facilitate equilibration. The Nafion samples in the NMR tubes were dried in a vacuum oven at 80 °C for 2 h; no residual water was observed by NMR after that drying treatment. Samples in the open NMR tubes were equilibrated at water activity from 0.05 to 0.9, and at 23, 50, and 70 °C in the environmental control chamber of the creep instrument. The times for equilibration were determined based on the membrane swelling measurements using the same apparatus.[19] Significantly longer time (5−30 h) was given in this set of experiments to ensure complete equilibration. Immediately after equilibration, NMR tubes containing strips of Nafion were quickly sealed at both ends by a plug and a positioning rod both made of Teflon, and then inserted into an insulated box before testing.

Pulse-field gradient spin echo NMR measurements were performed on a Varian Inova 500 spectrometer with a 5 mm z-gradient probe and temperature control. The samples were heated in the NMR spectrometer sample compartment to thermally reequilibrate for 30−60 min to the same temperature of the water absorption equilibration. The samples were tightly sealed so that the water activity would be the same as previously established. A stimulated echo pulse sequence was employed for the measurement.[20] Using bipolar pulse pairs, eddy currents induced by the gradients were minimized.[21] The radio frequency pulse width was calibrated for Nafion samples to obtain maximum signal intensity. Gradient pulses (g) were varied from 0.5 to 110.5 G/cm with 1 ms pulse width (δ). The spin echo signal decay can be related to water self-diffusion by eq 1,[20] from which self-diffusivity of water in Nafion was calculated, where I_0 and I are echo signal intensities at initial gradient and subsequent gradients, respectively; γ is the gyromagnetic ratio, and Δ is the duration of the diffusion experiments.

$$\frac{I}{I_0} = \exp\left[-D(\gamma g\delta)^2\left(\Delta - \frac{\delta}{3}\right)\right] \quad (1)$$

The logarithm of the intensity ratio ($\ln(I/I_0)$) was plotted as a function of the gradient strength, g, at fixed delay time to obtain

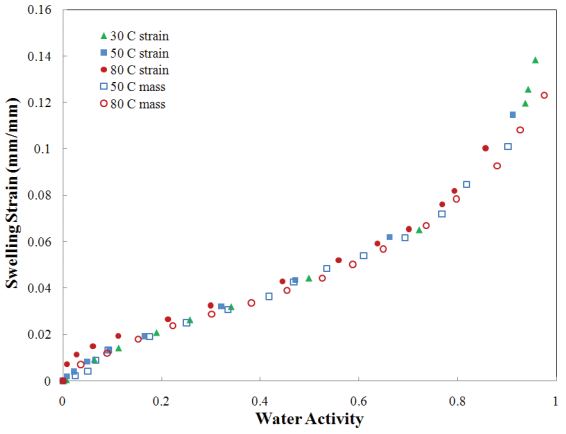

Figure 1. Linear swelling strain and ideal swelling strain based on water mass uptake of 1100 EW Nafion as a function of water activity at 30, 50, and 80 °C. The solid symbols are the experimentally measured linear swelling strain. The open symbols are the swelling strain predicted from water mass uptake assuming zero excess volume of mixing.

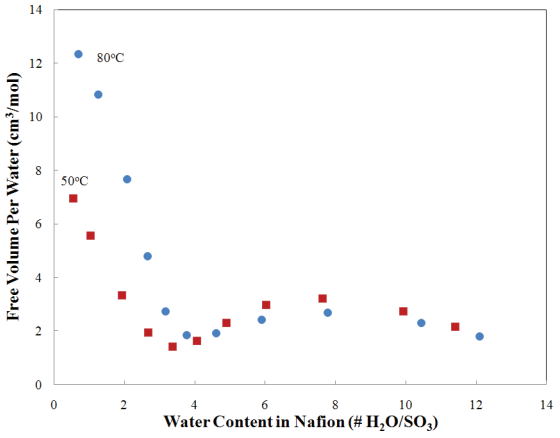

Figure 2. Free volume of water per water molecule as a function of $\lambda = \#H_2O/SO_3$ in 1100 EW Nafion. Data are shown for both 50 and 80 °C. Free volume was determined from polynomial fits of the swelling strain data and the ideal swelling strain data.

the diffusion coefficient. Diffusion coefficients were determined as Δ was varied from 10 to 2000 ms to obtain the limiting self-diffusivity, D_∞, of water; 3 to 4 samples were tested at each environmental condition, and each sample contained two pieces of identical Nafion strips to enhance signal intensity. The estimated error in determining D_∞ was $\sim 1 \times 10^{-7}$ cm^2/s. This was limited by the signal-to-noise ratio of the intensity at high gradient strength and was particularly sensitive to alkaline impurities in Nafion.

RESULTS

Equilibrium Water Absorption and Equilibrium Swelling Strain. Equilibrium water sorption (reported as $\lambda = \#H_2O/SO_3$) and equilibrium swelling strain $\varepsilon(\alpha_w)$ were measured as functions of temperature and water vapor pressure. At equilibrium, the activity of water in the membrane and in the vapor phase are the same and equal to the partial pressure (P_w) normalized by the vapor pressure of water (P_w^0) at the temperature of the measurement ($\alpha_w = P_w/P_w^0$). Membrane water activity scales with membrane water concentration (similar to water absorption into a solution). Figure 1 is a graph of the membrane water concentration as a function of water vapor activity, which shows the data at different temperatures may be superposed. Swelling strain depends on water sorption and scales with water activity, also evident in Figure 1.

The swelling strain for water absorption with perfect mixing corresponds to zero excess volume of mixing and can be determined from the equilibrium water sorption. The volume of water sorbed per unit volume of dry Nafion is given by $(\lambda\rho_{Nafion}\cdot MW_{water})/(EW\cdot\rho_{water})$ (ρ_{Nafion} and ρ_{water} are densities of Nafion and water, and MW_{water} is the molecular weight of water). The linear expansion coefficient, ε_0, for perfect mixing is given by eq 2.

$$(1+\varepsilon_0)^3 = \left(1 + \frac{\lambda\rho_{Nafion}MW_{water}}{EW\rho_{water}}\right) \quad (2)$$

The fractional excess volume change of water sorption (actual swelling minus swelling assuming perfect mixing) normalized by the initial membrane volume ($\bar{V}$) is given by eq 3. The excess volume change may be thought of as the free volume (V_f) associated with water sorption.

$$(1+\varepsilon)^3 - (1+\varepsilon_0)^3 = \frac{V_f}{\bar{V}} \quad (3)$$

It is most useful to consider the free volume per sorbed water molecule, which is given by eq 4, where N_w is the molar density of water.

$$\frac{V_f}{N_w} = \frac{(1+\varepsilon)^3[(1+\varepsilon)^3 - (1+\varepsilon_0)^3]}{\frac{\lambda\rho_{Nafion}}{EW}} \quad (4)$$

The free volume of water sorption per mole of water as a function of λ is shown in Figure 2. At 80 °C the free volume decreases from 12 cm^3/mol at $\lambda = 0.5$ ($a_w = 0.02$) to a value of $\sim$1.5 cm^3/mol at $\lambda = 4$ ($a_w = 0.5$). The free volume increases with λ to $\sim$3 cm^3/mol at $\lambda = 8$ ($a_w \sim 0.8$) and then decays toward zero with further increase of water uptake. At 50 °C the free volume per water molecule decreases from $\sim$7 cm^3/mol at $\lambda = 0.5$ to a value of 1 cm^3/mol at $\lambda = 4$. The free volume increases with λ going through a maximum at $\lambda = 8$ and then decreases toward zero.

Figures 1 and 2 suggest two stages to water sorption. (I) Water activity $0 < a_w < 0.5$: swelling strain increases ($\varepsilon > 0$), the rate of strain increase with water activity decreases ($(d^2\varepsilon/d\alpha_w^2)_I < 0$), and the free volume per water molecule decreases, $[d(V_f/N_w)/d\lambda]_I < 0$ with increased water activity. (II) $0.5 < a_w < 1.0$: swelling strain increases ($\varepsilon > 0$), the rate of strain increase with water activity increases ($(d^2\varepsilon/d\alpha_w^2)_{II} > 0$), and the free volume per water molecule is almost constant $[d(V_f/N_w)/d\lambda]_{II} \approx 0$. We suggest that the first stage of water sorption corresponds to the first solvation shell of the hydrophilic sulfonic acid groups. This is expected to involve strong bonding between the water and acid groups and is the reason why it is necessary to dry Nafion at 70−80 °C in vacuum for several hours to produce fully dry films. The second stage of water sorption forms a more weakly bound water (second solvation shell and beyond) which more closely resembles liquid water and creates much less free volume.

PGSE NMR. The hydrophilic domains of Nafion form a network within a hydrophobic matrix. Water is primarily transported through the hydrophilic network. Probing diffusion at

dx.doi.org/10.1021/jp1112125 |J. Phys. Chem. B 2011, 115, 2717–2727

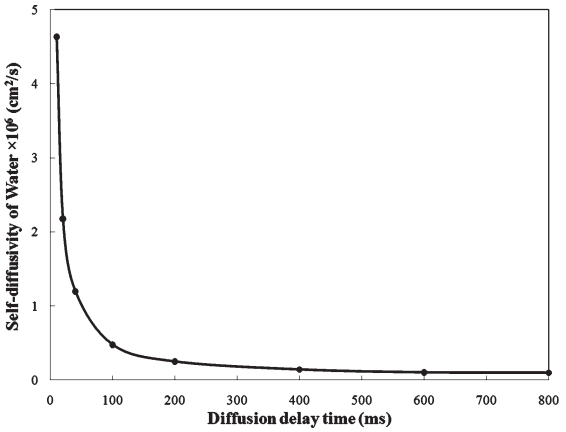

Figure 3. Decay of the self-diffusivity of water in 1100 EW Nafion with diffusion delay time at T = 23 °C and α_w = 0.1. At short delay time the diffusion coefficient is the molecular diffusivity. The effective diffusivity reflecting the tortuosity of the diffusion path through the hydrophilic domains is captured as delay time goes to ∞.

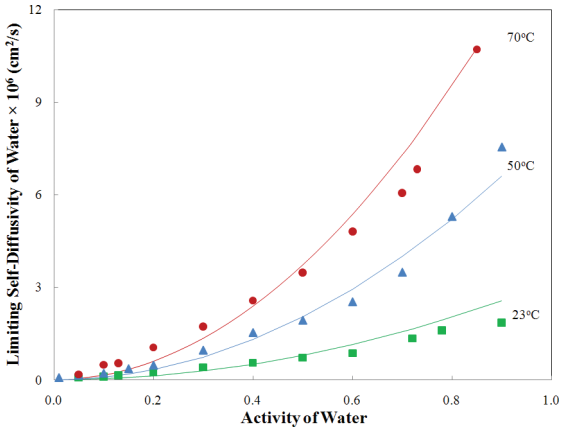

Figure 4. Limiting self-diffusivity of water (D_∞) in Nafion as a function of membrane water activity at 23, 50, and 70 °C. The standard error is below 10% for all data points. The data were fitted to an Arrhenius form to obtain a empirical equation $D_\infty = 0.265\alpha_w^2 e^{(-3343/T)}$ (cm^2/s), plotted as the smooth curves.

short times will only allow the water molecules to translate a short distance and they will not feel the restrictions of the tortuous network of the hydrophilic domain. The short time delay measurement is the molecular diffusivity D_m, where molecules only interact with near-neighboring molecules. Probing at longer times, the restrictions to diffusion imposed by size and tortuosity of the hydrophilic domains are sampled. As the delay time increases, the effective diffusion coefficient reaches a limiting value, D_∞, corresponding to where molecular diffusion is sufficient to permit the molecules to sample the entire interconnected hydrophilic domain.

Figure 3 is an example of the measured self-diffusivity of water in Nafion as a function of the pulse delay time, Δ, for samples with EDTA ion exchange. The effective self-diffusivity decreases from 4.5 × 10^{-6} cm^2/s when the delay time was 10 ms to a limiting value of 1.0 × 10^{-7} cm^2/s at delay times of ∼1000 ms. The decay of the effective diffusivity with delay time has been seen for liquid molecules in interconnected networks and porous medium.[22] The limiting self-diffusivity, D_∞, accounts for the volume fraction of the hydrophilic domain ($\varphi_{hydrophilic}$) and the tortuosity (τ) of the domain network is given by eq 5. Tortuosity is a measure of the connectivity of the hydrophilic domains. It represents the ratio of the length of the diffusion path through the hydrophilic domains to straight-line distance across the membrane.

$$D_\infty = D_m \frac{\varphi_{hydrophilic}}{\tau} \quad (5)$$

The molecular diffusivity can be determined from the effective self-diffusivity as the delay time approaches zero. The limiting diffusivity D_∞ is found for long delay times, Δ ≥ 1000 ms. The swelling experiments provide the measurement of $\varphi_{hydrophilic}$. Combining the NMR and swelling experiments, we can determine the tortuosity for water diffusion through the hydrophilic domains.

A critical experimental detail necessary to obtain accurate value of D_∞ is to minimize the magnetic dipolar coupling induced by unpaired electrons of the paramagnetic impurities, which significantly shortens the spin−lattice relaxation time (T_1).[23] The ion extraction with EDTA was essential to minimize the dipolar coupling with cations, such as Mg, Fe, etc., that can associate with the sulfonate groups. We observed that, without the EDTA ion exchange, T_1 is less than 20 ms, making it impossible to determining the limiting diffusivity; the spin echo signal was buried in the noise after 100 ms for all but the highest applied gradient fields.

Effective diffusivities were determined at pulse delay times of 10 ms (D_m) and 1000−2000 ms (D_∞) as functions of temperature and water activity. Diffusivites were in the range of 10^{-8}−10^{-6} for D_∞ to 10^{-5} cm^2/s for D_m. The characteristic length scale of a porous network that can be sampled during the delay is approximately $(2D_m\Delta)^{1/2}$.[24,25] Delay times of 1000 ms correspond to a molecular diffusion distance on the order of 50 μm, consistent with values reported in the literature,[25] and also the same magnitude as the Nafion membrane thickness. At delay times of 1000 ms the PGSE probes a distance that spans the membrane to allow determination of the effective diffusion coefficient across the membrane.

The limiting self-diffusivity of water in Nafion 1110 is displayed as a function of membrane water activity at three temperatures in Figure 4. At constant water activity, diffusivity increases by about a factor of 5 from 23 to 70 °C. In contrast, the diffusivity increases by 2 orders of magnitude with increasing water activity at constant temperature. Diffusion of solutes in polymers is often correlated with an exponential function of free volume. Figure 5 is a plot of ln(D_∞) as a function of λ. The self-diffusivity of water showed two regimes with a change in slope circa λ = 4.

$$\left.\frac{d \ln D_\infty}{d\varphi_{water}}\right|_{\lambda<4} > \left.\frac{d \ln D_\infty}{d\varphi_{water}}\right|_{\lambda>4} \quad (6)$$

The diffusivity shows a change in behavior at the same water volume fraction, or water activity where free volume per molecule of water also shows a change in behavior. We suggest the change in diffusivity is also associated with the binding of water to the HSO_3 groups. The waters in the first solvation shell more strongly interact with the sulfonic acid groups and display a reduced diffusivity. Subsequent water molecules are less strongly attached to the sulfonic acid group and diffuse more easily.

The tortuous network of hydrophilic domains reduces the effective diffusivity as indicated in eq 5. Both the molecular self-diffusion

dx.doi.org/10.1021/jp1112125 |J. Phys. Chem. B 2011, 115, 2717–2727

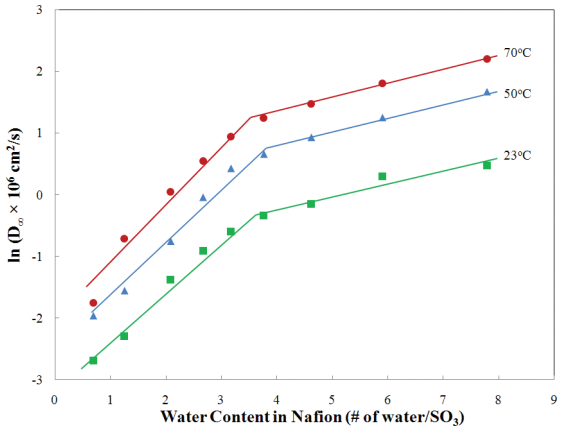

Figure 5. Plot of $\ln(D_s)$ vs membrane water content in Nafion at 23, 50, and 70 °C.

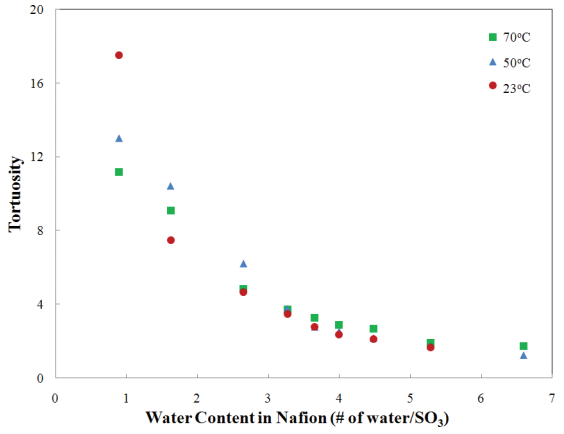

Figure 6. Tortuosity for water diffusion in Nafion as a function of water content in Nafion at 23, 50, and 70 °C.

coefficient and limiting self-diffusion coefficients were determined by PGSE NMR. The volume fraction of the hydrophilic domains can be determined from the volume of water sorbed and the volume fraction of dry Nafion assumed to be hydrophilic. If we assume that the sulfonic acid groups are the only hydrophilic species in dry Nafion, the volume fraction of the hydrophilic domains as a function of water activity is given by eq 7.

$$\varphi_{\text{hydrophilic}} = \frac{(1+\varepsilon)^3 - 1 + \phi_0}{(1+\varepsilon)^3} \qquad (7)$$

$\phi_0 = (\rho_{\text{Nafion}})/(\text{EW})\bar{V}_{SO_3}$ is the volume fraction of the hydrophilic phase in dry Nafion. The tortuosity of the hydrophilic domains can be evaluated by combining eqs 6 and 8 along with the values of D_m and D_∞. Figure 6 is a plot of the tortuosity as a function of λ. The tortuosity is very large, $\tau \sim 20$, at $\lambda = 0.5$ (low water activity) and decreases by an order of magnitude to approximately 2 at high λ ($\lambda > 5$).

DISCUSSION

Nafion is known to consist of two components that are strongly phase separating. In its dry state, there is a hydrophobic matrix consisting of a tetrafluoroethylene backbone and perfluoroalkyl ether side chains that account for ~90 vol % and very hydrophilic sulfonic acid groups that account for ~10 vol %.

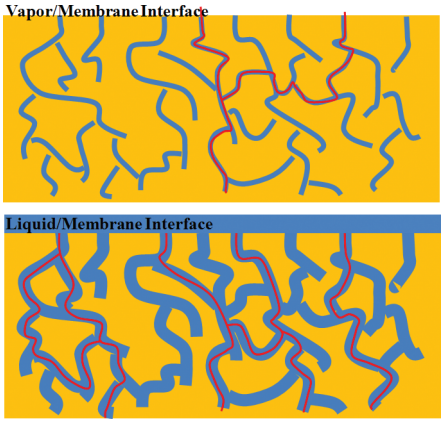

Figure 7. Schematic of hydrophilic network for water diffusion in Nafion. The figure at the top is at low water activity. The connectivity of paths across the membrane is low indicating a high tortuosity. At the bottom, hydrophilic domains are swollen from water sorption connecting different paths reducing tortuosity. The liquid/Nafion interface and vapor/Nafion interface indicate the differences in entry points for water molecules to enter the hydrophilic domains in the membrane.

Water interacts with the hydrophilic sulfonic acid groups; water sorption hydrates the sulfonic acid groups swelling the hydrophilic domains that are embedded in the hydrophobic matrix. Water sorption is limited by a balance of the energy of hydration of the sulfonic acid groups and the energy to swell the surrounding hydrophobic matrix.

Transport of water is confined to the hydrophilic domains. Water sorption swells the hydrophilic domains, creating greater volume for water to move, which increases the water diffusion rate. The experimental results reported here quantify how much the diffusion of water changes due to water sorption, and what the changes in diffusion coefficient indicate about the structure of the hydrophilic domains.

The key experimental findings reported above are as follows:

1. Water sorption occurs in two stages. A primary hydration shell of the sulfonic acid groups forms at low water activity ($a_w < 0.5$) with $\lambda \sim 4$ water molecules. At high water activity ($a_w > 0.8$), a second (and beyond) hydration shell forms.
2. The initial free volume of water sorption is large (>12 cm^3) and decreases with the number of molecules sorbed.
3. The effective or limiting water self-diffusion coefficients, at constant temperature, increase by a factor of 40 between low water activity ($a_w = 0.05$) and high water activity ($a_w = 0.90$). Self-diffusion coefficients, at constant water activity, increase by a factor of 5 as temperature increased from 23 to 70 °C.
4. The tortuosity for water diffusion decreased from 20 at low water activity to 2 at high water activity.
5. Free volume and self-diffusivity showed distinctive changes with water sorption above 4 water molecules sorbed per sulfonic acid group.

Many models of the microphase separation of Nafion have been published.[26,27] These have been generally based on scattering experiments and most often are done at variable water content. Transport property measurements provide information of the connectivity of the hydrophilic domains. The experimental findings of free volume, diffusion coefficients, and tortuosity reported here and our previous data on permeation rates provide

Table 1. Summary of Water Self Diffusion Coefficient in Nafion

researchers	conditions	results
	T = 30 °C	
Zawodzinski et al.[15]	λ = 2−14	$D = (0.6-5.8) \times 10^{-6}$ cm^2/s
	$\Delta \geq$ 20 ms	no change with Δ
	T not specified	
Tsushima et al.[14]	λ = 6−20	$D \sim (4-7.5) \times 10^{-6}$ cm^2/s
	Δ not specified	
	T = 25, 90 °C	
Hensley et al.[48]	RH = 100%	$D \sim 7 \times 10^{-6}$ cm^2/s at T = 25 °C
	Δ = 4.2 ms	$D \sim 27 \times 10^{-6}$ cm^2/s at T = 90 °C
	T = 40−80 °C	$D \sim (2-5.5) \times 10^{-6}$ cm^2/s at T = 40 °C
Kidena et al.[13]	RH = 40−80%	$D \sim (3-7.2) \times 10^{-6}$ cm^2/s at T = 60 °C
	Δ = 20 ms	$D \sim (3-10) \times 10^{-6}$ cm^2/s at T = 80 °C
	T = 22 °C	$D = 4.8 \times 10^{-6}$ cm^2/s
Ye et al.[49]	RH = 90% at 50 °C	no change with Δ
	Δ = 50−300 ms	
	T = 25 °C	$D \sim (1-7) \times 10^{-6}$ cm^2/s
Edmondson et al.[12]	water mass fraction = 0.04−0.2	no mention of Δ dependence
	Δ = 10−20 ms	
	T = 23−84 °C	
Gong et al.[50]	water mass fraction = 0.03−0.2	$D \sim 0.2-20 \times 10^{-6}$ cm^2/s
	Δ = 3−600 ms	no mention of Δ dependence
	T = −40−35 °C	
Ohkubo et al.[25]	λ = 4 and 15	D decreases with Δ = 1 to 2 ms and becomes constant beyond that
	Δ = 1−100 ms	
	T = 25 °C	$D \sim (2-3) \times 10^{-6}$ cm^2/s
Roy et al.[51]	fully saturated with water	D decreases from Δ = 10 to 20 ms and states constant beyond that
	Δ = 10−80 ms	

the following insights into the structure of the hydrophilic domains.

1. Water coordinates around sulfonic acid groups. A first hydration shell of 4 water molecules forms.
2. The connectivity of the hydrophilic domains increases with water sorption.
3. There are few hydrophilic domains that extend to the Nafion/vapor interface, more hydrophilic domains extend to the Nafion/liquid water interface.

These results suggest a model for the hydrophilic domains shown in Figure 7. The hydrophilic domains are channels of sulfonic acid groups with waters of hydration spread throughout the hydrophobic matrix. (Channels could be lamella, rods, or spherical clusters). These channels are hydrophilic with high surface energy. When the exterior membrane surface is in contact with a vapor, the surface energy is minimized by having the channels buried beneath the surface. In contrast, liquid water at the external membrane surface will prefer having the hydrophilic channels extend to the interface. Water sorption increases the sizes of the channels and their connectivity. The increased number of continuous paths across the membrane (shown as red lines in Figure 7) at the higher water content results in reduced tortuosity.

Experimental Challenges Measuring Water Diffusion in Nafion Membranes. Water transport in Nafion has been studied by many different techniques, and diffusion coefficients reported vary by orders of magnitude and depend on the method of measurements. NMR measures the self-diffusivity of water in the membrane, but the method poses complications in controlling water activity. Table 1 summarizes recent NMR studies employed to measure water transport in Nafion. The studies that employed PGSE reported larger diffusion coefficients than the limiting self-diffusivities we determined. A number of the reported D values were obtained after short delay times of 20 ms, which are much shorter delay times than we employed to get D_∞. Some investigators claimed that the diffusivity was independent of the delay time. We cannot account for all the experimental details from these previous studies, but we identified two important experimental details that were critical to obtain reproducible results: (1) it was critical to remove paramagnetic metal cation impurities that can cause dipolar coupling; and (2) it was essential to properly control the water activity.

Only one previous study specifically mentioned ion exchange with EDTA to prepare the Nafion. The removal of the cation impurities permitted measurements with much longer delay times which were required to reach D_∞. We took data for a few samples that had not been ion exchanged. Without ion exchange, the NMR peaks were buried in the noise for all but the shortest pulse delay times. We believe this was due to dipolar coupling with alkali cations causing dephasing of the proton spins. Without ion exchange, data could only be obtained at the shortest delay times, making it impossible to obtain the limiting diffusivity. Only the molecular diffusivity for small displacements could be accurately measured without ion exchange.

Our experiments were done at fixed water vapor activity. Many researchers have attempted to carry out studies with fixed water content. Equilibrating a membrane and vapor in a closed volume at one temperature fixes the total water inventory. Temperature

changes will result in water repartitioning between the membrane and the vapor phase to establish water activity equilibrium. Samples should be fully equilibrated at the same temperature and water activity as the measurement. Water vapor activity can be controlled with saturated salt solutions or mixed humidified and dry gas streams. We found direct control of the vapor activity by mixing a nearly saturated vapor stream with a dry stream of N_2 was more effective. With salt solutions we experienced slow equilibration between the salt solution and the vapor that contributed to uncertainty in the water activity.

Water Sorption and Free Volume. A number of studies of water uptake by Nafion report similar results to those presented in Figure 1.[28] Many investigators have also reported Nafion's volume change for a dry film placed into liquid water. Data reported here is the first systematic reporting of the swelling of Nafion as a function of water activity.

Independent measurements of water uptake and linear expansion provide a direct determination of the excess volume of mixing associated with water sorption in Nafion. Positive excess volume of mixing means that sorbed water creates free volume which should permit more facile diffusion. The free volume for the initial water sorption at 80 °C is 12 cm^3/mol, which is 2/3 the molar volume of liquid water; this indicates that the initial water sorption requires almost twice the volume of the water molecules. The water being sorbed must be severely disrupting the packing of the Nafion molecules. Figure 8 suggests how this might occur in a hydrophilic channel of Nafion. In the dry state the sulfonic acid groups of Nafion would become interdigitated by electrostatic dipole interactions. Coordination of a water molecule to a sulfonic acid group pushes the sulfonic acid groups apart and creates a void. As more water molecules are absorbed, the packing would become more efficient and the free volume per molecule decreases. There is a change in slope of the free volume per water at $\lambda = 4$ water molecules per sulfonic acid group, which we suggest is the first hydration shell around a sulfonic acid group. Subsequent water addition is in the second hydration shell and beyond, where the interactions between water molecules are approaching the interactions of bulk water.

The data in Figure 2 shows an increase in the free volume from $\lambda = 4$ to $\lambda = 8$, and then the free volume decreases toward zero at larger water uptake. We suggest this change in free volume is the result of changes to the microstructural topology of the hydrophilic domains. Majsztrik et al. observed a minima in the tensile creep of Nafion at $\lambda = 8$ where the secondary maximum in free volume occurs. They attributed the minima in tensile creep rate to a change in the topology of the hydrophilic domains; they suggested it corresponded to a change from a lamellar to a cylindrical structure of the hydrophilic domains.[29] Changes in the microstructure of the hydrophilic domains would be expected to alter the molecular packing and hence the free volume.

Some investigators have suggested that the hydrophilic domains in Nafion formed a porous network and water adsorbed onto the walls of the hydrophilic channels.[30,31] If pores existed where water could adsorb onto free surfaces, the fractional excess volume change would be negative; the water would be sorbed without volume change. This is contrary to the results presented in Figures 1 and 2.

Rather than water adsorption on free surfaces, water sorption could be considered to be analogous to multilayer adsorption, where hydration shells about the sulfonic acid groups are like adsorbed molecules on adsorption sites. The first solvation shell is the equivalent of the monolayer, except the adsorption site

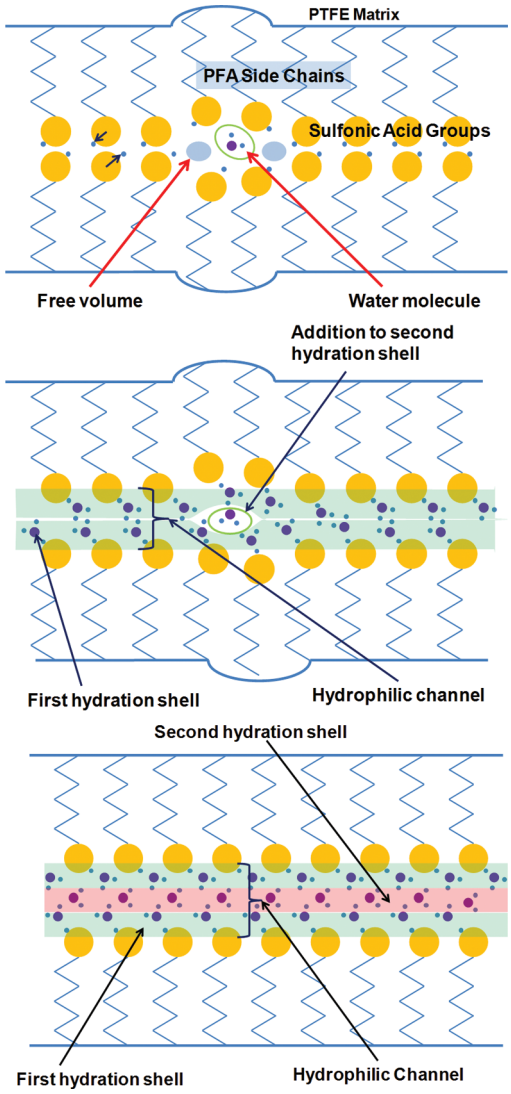

Figure 8. Schematic of microphase separation in Nafion. The TFE and PFA form a hydrophobic matrix. Sulfonic acid groups cluster and absorb water forming hydrophilic pores. Water is transported through hydrophilic domains. (a, upper) In the absence of water the sulfonic acid dipoles will attempt to interdigitate forming a hydrophilic channel. Water absorbed in the channel will disrupt the packing creating free volume as it pushes upon the hydrophobic matrix to allow incorporation. (b, middle) A first solvation shell of water forms with each sulfonic acid residue surrounded with water dipoles to shield the dipole of the sulfonic acid. Additional water absorb with weaker interactions and less disruption of the structure. (c, lower) Additional water absorbs into the hydrophilic channel in a second solvation shell.

(e.g., the sulfonic acid) can accommodate several adsorbates (water molecules) in the monolayer.

Correlation of Diffusion and Free Volume. Diffusion in condensed phases requires defects in molecular packing of the molecules. In polymers, the imperfect packing associated with glassy or liquidlike structure permits small molecules to move through the polymer network. The imperfect packing creates nanometer voids generally referred to as free volume; the greater the free volume the more facile is diffusion. Theories of diffusion in polymers often relate the diffusivity to the free volume.[32,33]

The slope of $\ln(D_\infty)$ vs λ changes at $\lambda = 4$. There is also a change in slope of tortuosity vs λ at $\lambda = 4$. We suggest that the

physical interaction between water and the sulfonic acid groups and the connectivity of the hydrophilic domains both contribute to the rate of change in diffusivity. (1) The strength of the electrostatic interactions between sulfonic acids and water molecules will decrease between the first hydration shell and subsequent hydration shells. The weaker electrostatic interactions between sulfonic acid groups and the second hydration shell permit more facile motion of water. (2) The connectivity of the hydrophilic network appears to be more fully established after the first 4 waters per sulfonic acid are sorbed. The tortuosity decreased from 20 to 2 indicating that water molecules could take a more direct path through the hydrophilic domains increasing the effective diffusivity. Structural changes in the topology of the hydrophilic domains, as suggested by Majsztrik et al., may also contribute the decrease in tortuosity.

Compositional Dependent Diffusivity. The effective self-diffusivity D_∞ is a function of both activity and temperature. The effective diffusivity data for EW 1100 Nafion was fit to $D_\infty = (D_0)\alpha_w^2 \exp(-E/RT)$, where $D_0 = 0.265$ cm^2/s, and $E = 28$ kJ/mol. The quadratic form was chosen empirically and found to be the lowest order polynomial that can fit the data reasonably well. The 36 experimental data points of D_∞ at three different temperatures and 12 different water activities were regressed to the two parameters D_0 and E. The fits to the data are shown in Figure 4. This is a convenient functional form for modeling transport of water in Nafion.

Water transport is associated with gradients in water activity. In the presence of gradients in water activity mutual diffusion coefficient (D_{mutual}) should be employed in place of the self-diffusion coefficient.[34,35] When the flux is written in terms of concentrations, the correction to the mutual diffusion coefficient must account for the activity coefficient, γ, as a function of water activity as shown in eq 8.

$$D_{mutual} = \frac{D_\infty}{RT}\left(\frac{\partial \mu_w}{\partial \ln C}\right)_{T,P} = \left(\frac{\partial \alpha_w}{\partial C}\right)\frac{C_0 D_\infty}{\gamma} \quad (8)$$

The activity coefficient is the ratio of the actual water concentration to the water concentration assuming an ideal solution. $C(\alpha_w)$ is the concentration of water in the hydrophilic phase, given by eq 9.

$$C_0 = \frac{\lambda \rho_{Nafion}}{EW \cdot [(1+\varepsilon)^3 - 1 + \phi_0]} \quad (9)$$

The standard-state concentration C_0 is taken as the concentration of water in the hydrophilic phase at activity equal to unity. A cubic equation was fit to the water uptake data and to evaluate the activity coefficient (eq 10).

$$\gamma = \frac{\alpha_w C_0}{C(\alpha_w)} \approx -1.9\alpha_w^3 + 2.5\alpha_w^2 + 0.1\alpha_w + 0.3 \quad (10)$$

In principle, the mutual diffusion coefficient should also account for the counter diffusion of the polymer, but the polymer chains are virtually immobile relative the water molecules.

Diffusion with Dimensional Change. Water sorption and water transport is almost exclusively restricted to the hydrophilic phase.[26] Water sorption swells the hydrophilic phase of Nafion, increasing the volume available for water transport. Majsztrik et al.[10] and Kusoglu et al.[36] have derived expressions relating the volume change of the hydrophilic domains to the linear expansion coefficient of Nafion due to water absorption. The linear expansion of the hydrophilic phase ε^*, is given by eq 11, assuming cylindrical channels.[37] The linear expansion of the hydrophilic domains is much greater than the linear expansion of the entire membrane ε. In fact, a 40% expansion of Nafion due to water absorption results in a 600% volume expansion of the hydrophilic domain.

$$\varepsilon^*(\alpha_w) = \left[\left(\frac{[1+\varepsilon(\alpha_w)]^3 - 1}{\phi_0} + 1\right)\frac{1}{(1+\varepsilon(\alpha_w))}\right]^{1/2} - 1 \quad (11)$$

Diffusion through the hydrophilic domains is increased due to the increased fractional area of the hydrophilic domains $(1+\varepsilon^*)^2$, and is decreased by the increased path length through the membrane for diffusion $(1+\varepsilon)$. The overall geometric correction for water transport is given by eq 12.

$$A_c = \frac{(1+\varepsilon^*)^2}{(1+\varepsilon)} = \frac{(1+\varepsilon)^3 - 1 + \phi_0}{\phi_0(1+\varepsilon)^2} \quad (12)$$

The diffusive water flux in the Nafion membrane is given by eq 13. Water diffusion is restricted to the hydrophilic domains; the concentration of water in the hydrophilic domains at water activity unity is given by eq 9.

$$\text{flux} = -A_c(\alpha_w)D_m(\alpha_w, T)\frac{\partial C}{\partial x} = -A_c C_0\left(\frac{D_\infty}{\gamma}\right)\frac{\partial \alpha_w}{\partial x} \quad (13)$$

Determination of Interfacial Mass Transport Coefficients. Majsztrik et al. had measured water permeation rates through Nafion and estimated diffusion coefficients and interfacial transport coefficients by assuming simple Fickian diffusion with constant diffusion coefficient across the membrane. With the improved knowledge of the diffusion coefficient's dependence on water activity, more accurate values of interfacial transport coefficients may be obtained.

Steady-state water permeation process through Nafion membranes can be broken down to three steps: (1) sorption of water into the membrane at the feed side, (2) diffusion of water across the membrane, and (3) desorption of water from the membrane into the dry gas flow. Steps 1 and 3 pose interfacial resistances. The hydrophobicity of the membrane surface, the change in phase of water at the interface, and a gas-phase boundary layer will contribute to the interfacial resistance. Elabd and coworkers[38] have looked more carefully at the gas-phase boundary layer resistance due to flow and found a small, but measurable effect. At the high gas flow limit employed in the permeation cell experiments reported by Majsztrik et al., the gas-side mass transport resistance may be neglected.

The microscopic details of the interfacial structure and composition are too complex to quantitatively model the interfacial transport from first principles. A lumped mass transport coefficient k_m that is correlated with temperature and water activity is employed to describe the rate of interfacial transport as shown in eq 14.

$$\text{flux} = k_m(\alpha_w^m - \alpha_w^{N_2}) \quad (14)$$

Wetting experiments have shown that the Nafion surface is hydrophobic when contacting water vapor, but becomes hydrophilic when contacting liquid water.[10,39−42] Possible polymer chain restructuring at the surface has been proposed.[40] Recently, Bass et al. used glazing-incident SAXS and observed rearrangements

of the hydrophobic chain bundles on Nafion surface to minimize surface energy when the membrane is in contact with water vapor.[43] In the same paper, Bass et al. also reported that Nafion surface exposed to fully saturated water vapor has nearly the same hydrophobicity as a completely dry membrane, which implies that Nafion's surface composition is enriched with hydrophobic domains and is not sensitive to water vapor activity. The hydrophobic Nafion/vapor interface creates a thin barrier that limits water transport.

In contrast, when Nafion is exposed to liquid water the interfacial energy will be minimized when the hydrophilic domains are drawn to the water/membrane interface. In addition, the collision rate of water molecules with the surface is much greater for a liquid than for a vapor. We suggest that water activity at liquid water/Nafion interface is equilibrated and the activity of water at the membrane interface is unity.

Water flux measurements were previously reported by Majsztrik et al. for liquid water on one side of Nafion 1100 EW membranes of different thickness. Knowing the water activity at the liquid/membrane interface, the water flux and the diffusion coefficient as a function of water activity, the diffusion equation (eq 13) can be integrated from the liquid/Nafion interface to the vapor/Nafion interface to determine the water activity at the vapor/Nafion interface (α_w^m). The water activity in the vapor phase ($\alpha_w^{N_2}$) was measured experimentally so the interfacial mass transport coefficient, k_m, can be evaluated from the water flux, the membrane water activity, and the vapor water activity at the membrane vapor interface.

Figure 9 illustrates the calculated water activity profiles for steady-state permeation of water through different Nafion membrane thicknesses with a liquid feed at 30 °C. The calculated profiles assume the water activity in the membrane at the liquid water/membrane interface is equal to 1 and the water flux is that determined from the experiments of Majsztrik et al.[10] Water activity stays high across the entire membrane at all three thicknesses, indicative of fast diffusion. At the vapor/membrane interface, the large drop in water activity indicates a large interfacial resistance. The ratio of the driving forces for diffusion to interfacial transport may be approximated by the ratio of the activity differences across the membrane to the activity difference across the interface. For the Nafion 1110 membrane this ratio is 0.6/0.2 = 3.

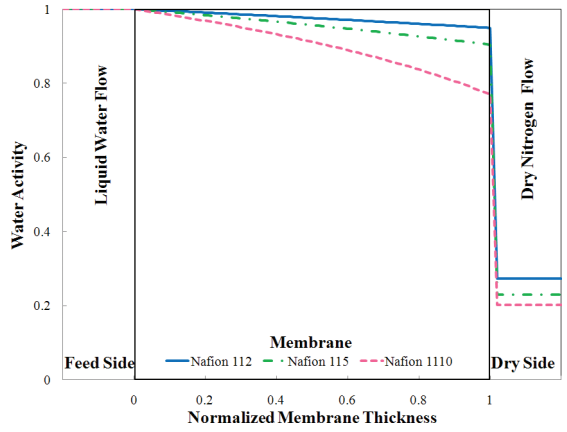

Figure 9. Water activity profiles for steady state permeation across Nafion 112, 115, and 1110 from liquid water at 30 °C. The profiles were calculated from the flux data and assuming the activity at water/membrane interface is unity. The dry side activity data were measured by Majsztrik.[19] The width of the interface on the dry side was randomly chosen only for the purpose of display.

Table 2 summarizes the water transport rate across Nafion 1110 from 30 to 70 °C, the water evaporation rate from liquid water ($r_{evaporation} = (2\pi M_w RT)^{1/2} P_w^0$), the ratio of water transport rate to ideal evaporation rate, and the interfacial mass transport coefficient. The water transport rate is 10^4 less than the evaporation from a film of water indicating a low efficiency of interfacial exchange at the vapor/membrane interface. The low interfacial transport rate is the result of a very small fraction of hydrophilic domains at the membrane/vapor surface available for water transport.

Knowing interfacial transport coefficients, diffusion coefficients, water activity coefficients, and the volumetric expansion coefficients as functions of temperature and water activity, the permeation rates through Nafion membranes and water activity profiles across Nafion membranes may be predicted. The predicted water transport rates with water vapor feeds are compared to the experimental rates determined by Majsztrik et al. in Table 3. In six of nine cases the model predictions differ from the experimental rates by less than 10% and the largest discrepancies were 40%. The model assumed that the interfacial transport coefficients were independent of water activity; the agreement of the model and experiment justify that assumption.

Figure 10 shows the predicted water activity profiles based on 50% RH vapor at the feed side of the membrane. Nafion 1110, which should have the largest diffusional resistance. The water activity difference at both vapor/membrane interfaces is 0.05 (0.5−0.45 at feed side and 0.06−0.01 at dry side). The water

Table 3. Permeation Rate from Water Vapor at 30 °C

feed side activity	flux (mol/cm^2/s)	Nafion 112	Nafion 115	Nafion 1110
0.3	experimental[a]	7.7×10^{-7}	5.3×10^{-7}	1.8×10^{-7}
	model prediction	7.8×10^{-7}	5.5×10^{-7}	3.2×10^{-7}
0.5	experimental[a]	1.5×10^{-6}	1.1×10^{-6}	9.0×10^{-7}
	model prediction	1.8×10^{-6}	1.5×10^{-6}	1.0×10^{-6}
0.8	experimental[a]	3.7×10^{-6}	2.5×10^{-6}	2.0×10^{-6}
	model prediction	4.0×10^{-6}	3.5×10^{-6}	2.6×10^{-6}

[a] Experimental error on flux measurements is estimated to be ±10%.

Table 2. Permeation Rates across Nafion 115 and Water Evaporation Rate

T (°C)	permeation rate (μmol/cm^2/s)	P_w^0 (bar)	water evaporation rate (mmol/cm^2/s)	permeation rate/evaporation rate	k_m (mol/cm^2/s)
30	7.4	0.042	25	3×10^{-4}	2.58×10^{-5}
50	14	0.122	73	2×10^{-4}	4.48×10^{-5}
70	23	0.308	184	1×10^{-4}	6.79×10^{-5}
80	28	0.467	279	1×10^{-4}	

dx.doi.org/10.1021/jp1112125 |J. Phys. Chem. B 2011, 115, 2717–2727

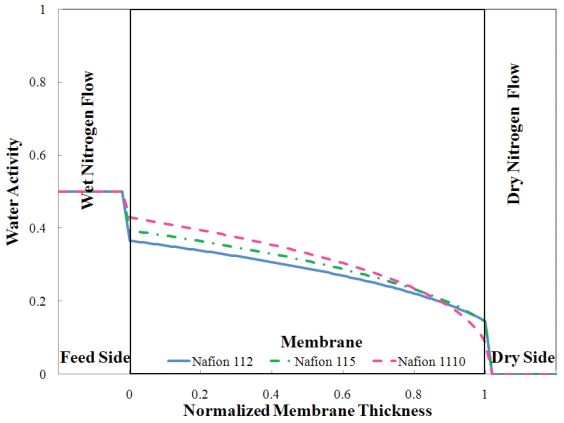

Figure 10. Water activity profiles for steady state permeation across Nafion 112, 115, and 1110 from $\alpha_w = 0.5$ vapor at 30 °C. The interfacial transport coefficients are reported in Table 2.

activity difference across the membrane is 0.39. The ratio of driving forces for diffusion/interfacial transport is 0.05/0.39 = 0.13. The ratio of the driving forces for diffusion to interfacial water transport with a vapor feed is 25 times greater than the ratio for a liquid feed. The difference in driving force for diffusion to interfacial transport reflects the shift in the rate-limited step for water permeation between diffusion at low membrane water activity to interfacial transport at high membrane water activity.

Implications of the Results for PEM Fuel Cell Operation. The results for water transport across Nafion membranes reported here are important for understanding the membrane water content in a running fuel cell. In a fuel cell, liquid water is produced at the cathode catalyst layer close to the membrane surface. The presence of liquid water at the cathode side of the membrane surface permits high diffusion rates of water from cathode to anode. The interfacial mass transport resistance at the membrane/vapor interface at the anode keeps the water activity in the membrane high. The high hydration is essential to maintain high proton conductivity in the Nafion membrane.

The results reported here for diffusion coefficients and interfacial transport coefficients may be employed to integrate the diffusion equation and understand the dynamics of water absorption and desorption reported in various experimental situations and water profiles imaged in fuel cells using NMR and neutron scattering. We have included as Supporting Information a compilation of analyses listed below:

1. Dynamics of water absorption and desorption from Nafion films. These have been compared to the experimental results of Satterfield and Benziger.[9]
2. Comparison of the dynamics of water absorption from liquid water and water vapor and its relation to Schroder's paradox. These results help understand the analysis of Onishi et al. who showed that the dynamics of water absorption from liquid water are much faster than absorption from saturated vapor.[44]
3. Steady-state water activity profiles in conditions simulating fuel cell operation. The steady-state profiles obtained by NMR imaging show almost uniform water composition across the membrane.[45] The model presented here explains those results.

The most important consequence of these results is that interfacial mass transport at the vapor/membrane interface limits water uptake dynamics by Nafion. Consequently, water absorption is more than 2 orders of magnitude slower from saturated vapor than saturated liquid. This difference in water absorption from saturated liquid and saturated vapor has puzzled researchers for a long time.[4−6,30,46,47]

Water absorption is also slower than water desorption.[9] Water content in the membrane starts high during desorption and low during absorption. Because water diffusivity increases significantly with membrane water content, water diffusion to/from the interface is faster during desorption than absorption.

The simulations presented in the Supporting Information show that proper accounting for activity-dependent diffusion coefficients and interfacial transport identify the rate-limiting step for water transport in Nafion and unify the experimental observations from different experiments.

CONCLUSION

Water diffusivity, interfacial mass transport, and volume available for transport are three critical factors that control the transport of water in Nafion membranes. These factors were quantified as functions of water activity and temperature by water sorption, volumetric expansion, pulsed gradient-spin echo NMR and steady-state permeation measurement.

A novel method of direct measurement of free volume associated with water absorption in Nafion is presented. The free volume is large for the first water molecules absorbed. The free volume per water molecule decreases for the first four water molecules absorbed. Self-diffusion coefficients were measured by PGSE-NMR at long delay times that captured the tortuous pore network of the hydrophilic domains in Nafion. At low membrane water activities, the tortuosity is large, resulting in a small effective diffusion coefficient for water.

The self-diffusion coefficients increased with water activity, showing two regimes. Diffusion coefficients increased rapidly with increased water for the first four water molecules per sulfonic acid, and then increased more slowly for water activities corresponding to more the four water molecules per sulfonic acid. The water sorption and diffusion results suggest four water molecules form a first solvation shell around the sulfonic acid groups. Beyond the first four water molecules, the diffusivity increases more rapidly with water sorption.

Interfacial mass transfer coefficients were evaluated for water transport across the Nafion/vapor interface. Results show that at high membrane water activity diffusion is fast and water transport is limited by interfacial transport at the membrane/vapor interface. At lower membrane water content the diffusion coefficient becomes smaller and diffusion becomes slower than vapor/membrane interfacial transport.

Incorporation of the concentration-dependent diffusivity, swelling of hydrophilic domains, and vapor/membrane interfacial transport into the diffusion equation allows for successful modeling of the dynamic water sorption/desorption in Nafion.

ASSOCIATED CONTENT

Supporting Information. Model predictions of the dynamics of water sorption and desorption from water vapor and water liquid and steady-state profiles of membrane water activities in fuel cells. This material is available free of charge via the Internet at http://pubs.acs.org.

AUTHOR INFORMATION

Corresponding Author
*E-mail: benziger@princeton.edu. Phone: 01-609-258-5416. Fax: 01-609-258-0211.

ACKNOWLEDGMENT

This work was supported by the National Science Foundation MRSEC Program through the Princeton Center for Complex Materials NSF DMR-0819860. We also thank Dr. Carlos Pacheco at the Department of Chemistry, Princeton University, for all the help and fruitful discussions for the NMR experiments.

REFERENCES

(1) Ge, S.; Li, X.; Yi, B.; Hsing, I. *J. Electrochem. Soc.* **2005**, *152*, A1149.
(2) Majsztrik, P. W.; Satterfield, M. B.; Bocarsly, A. B.; Benziger, J. B. *J. Membr. Sci.* **2007**, *301*, 93.
(3) Zawodzinski, T. A.; Derouin, C.; Radzinski, S.; Sherman, R. J.; Smith, V. T.; Springer, T. E.; Gottesfeld, S. *J. Electrochem. Soc.* **1993**, *140*, 1041.
(4) Rivin, D.; Kendrick, C. E.; Gibson, P. W.; Schneider, N. S. *Polymer* **2001**, *42*, 623.
(5) Takamatsu, T.; Hashiyama, M.; Eisenberg, A. *J. Appl. Polym. Sci.* **1979**, *24*, 2199.
(6) Morris, D. R.; Sun, X. D. *J. Appl. Polym. Sci.* **1993**, *50*, 1445.
(7) Krtil, P.; Trojanek, A.; Samec, Z. *J. Phys. Chem. B* **2001**, *105*, 7979.
(8) Burnett, D. J.; Garcia, A. R.; Thielmann, F. *J. Power Sources* **2006**, *160*, 426.
(9) Satterfield, M. B.; Benziger, J. B. *J. Phys. Chem. B* **2008**, *112*, 3693.
(10) Majsztrik, P.; Bocarsly, A.; Benziger, J. *J. Phys. Chem. B* **2008**, *112*, 16280.
(11) Monroe, C. W.; Romero, T.; Merida, W.; Eikerling, M. *J. Membr. Sci.* **2008**, *324*, 1.
(12) Edmondson, C. A.; Fontanella, J. J.; Chung, S. H.; Greenbaum, S. G.; Wnek, G. E. *Electrochim. Acta* **2001**, *46*, 1623.
(13) Kidena, K.; Ohkubo, T.; Takimoto, N.; Ohira, A. *Eur. Polym. J.* **2010**, *46*, 450.
(14) Tsushima, S.; Teranishi, K.; Hirai, S. *Energy* **2005**, *30*, 235.
(15) Zawodzinski, T. A.; Neeman, M.; Sillerud, L. O.; Gottesfeld, S. *J. Phys. Chem.* **1991**, *95*, 6040.
(16) MacMillan, B.; Sharp, A. R.; Armstrong, R. L. *Polymer* **1999**, *40*, 2471.
(17) Yang, C.; Srinivasan, S.; Bocarsly, A. B.; Tulyani, S.; Benziger, J. B. *J. Membr. Sci.* **2004**, *237*, 145.
(18) Majsztrik, P. W.; Bocarsly, A. B.; Benziger, J. B. *Rev. Sci. Instrum.* **2007**, *78*, 3904.
(19) Majsztrik, P. W. *Mechanical and Transport Properties of Nafion for PEM Fuel Cells; Temperature and Hydration Effects*; Princeton University: Princeton, NJ, 2008.
(20) Cotts, R. M.; Hoch, M. J. R.; Sun, T.; Markert, J. T. *J. Magn. Reson.* **1989**, *83*, 252.
(21) Wu, D. H.; Chen, A. D.; Johnson, C. S. *J. Magn. Reson. Ser. A* **1995**, *115*, 260.
(22) Callaghan, P. T. *Principles of Nuclear Magnetic Resonance Microscopy*; Oxford University Press: New York, 1991.
(23) Phua, T. T.; Beaudry, B. J.; Peterson, D. T.; Torgeson, D. R.; Barnes, R. G.; Belhoul, M.; Styles, G. A.; Seymour, E. F. W. *Phys. Rev. B* **1983**, *28*, 6227.
(24) Callaghan, P. T.; Coy, A.; Halpin, T. P. J.; Macgowan, D.; Packer, K. J.; Zelaya, F. O. *J. Chem. Phys.* **1992**, *97*, 651.
(25) Ohkubo, T.; Kidena, K.; Ohira, A. *Macromolecules* **2008**, *41*, 8688.
(26) Mauritz, K. A.; Moore, R. B. *Chem. Rev.* **2004**, *104*, 4535.
(27) Gebel, G. *Polymer* **2000**, *41*, 5829.
(28) Jalani, N. H.; Choi, P.; Datta, R. *J. Membr. Sci.* **2005**, *254*, 31.
(29) Majsztrik, P. W.; Bocarsly, A. B.; Benziger, J. B. *Macromolecules* **2008**, *41*, 9849.
(30) Choi, P. H.; Datta, R. *J. Electrochem. Soc.* **2003**, *150*, E601.
(31) Choi, P.; Jalani, N. H.; Datta, R. *J. Electrochem. Soc.* **2005**, *152*, E84.
(32) Vrentas, J. S.; Duda, J. L. *J. Polym. Sci., B: Polym. Phys.* **1977**, *15*, 403.
(33) Zielinski, J. M.; Duda, J. L. *AICHe J.* **1992**, *38*, 405.
(34) Duda, J. L.; Ni, Y. C.; Vrentas, J. S. *Macromolecules* **1979**, *12*, 459.
(35) Weppner, W.; Huggins, R. A. *J. Electrochem. Soc.* **1977**, *124*, 1569.
(36) Kusoglu, A.; Santare, M. H.; Karlsson, A. M.; Cleghorn, S.; Johnson, W. B. *J. Polym. Sci., B: Polym. Phys.* **2008**, *46*, 2404.
(37) Schmidt-Rohr, K.; Chen, Q. *Nat. Mater.* **2008**, *7*, 75.
(38) Hallinan, D. T.; Elabd, Y. A. *J. Phys. Chem. B* **2009**, *113*, 4257.
(39) Freger, V. *J. Phys. Chem. B* **2009**, *113*, 24.
(40) Goswami, S.; Klaus, S.; Benziger, J. *Langmuir* **2008**, *24*, 8627.
(41) Zawodzinski, T. A.; Springer, T. E.; Uribe, F.; Gottesfeld, S. *Solid State Ionics* **1993**, *60*, 199.
(42) Yu, H. M.; Ziegler, C.; Oszcipok, M.; Zobel, M.; Hebling, C. *Electrochim. Acta* **2006**, *51*, 1199.
(43) Bass, M.; Berman, A.; Singh, A.; Konovalov, O.; Freger, V. *J. Phys. Chem. B* **2010**, *114*, 3784.
(44) Onishi, L. M.; Prausnitz, J. M.; Newman, J. *J. Phys. Chem. B* **2007**, *111*, 10166.
(45) Zhang, Z.; Martin, J.; Wu, J.; Wang, H.; Promislow, K.; Balcom, B. J. *J. Magn. Reson.* **2008**, *193*, 259.
(46) Bass, M.; Freger, V. *Polymer* **2008**, *49*, 497.
(47) Hinatsu, J. T.; Mizuhata, M.; Takenaka, H. *J. Electrochem. Soc.* **1994**, *141*, 1493.
(48) Hensley, J. E.; Way, J. D.; Dec, S. F.; Abney, K. D. *J. Membr. Sci.* **2007**, *298*, 190.
(49) Ye, G.; Hayden, C. A.; Goward, G. R. *Macromolecules* **2007**, *40*, 1529.
(50) Gong, X.; Bandis, A.; Tao, A.; Meresi, G.; Wang, Y.; Inglefield, P. T.; Jones, A. A.; Wen, W. Y. *Polymer* **2001**, *42*, 6485.
(51) Roy, A.; Hickner, M. A.; Yu, X.; Li, Y. X.; Glass, T. E.; McGrath, J. E. *J. Polym. Sci., B: Polym. Phys.* **2006**, *44*, 2226.